the plant journal

SEB Society for Experimental Biology

The Plant Journal (2012) **72**, 355–367 doi: 10.1111/j.1365-313X.2012.05086.x

FEATURED ARTICLE

Soybean ureide transporters play a critical role in nodule development, function and nitrogen export

Ray Collier and Mechthild Tegeder*

School of Biological Sciences, Washington State University, Pullman, WA 99164-4236, USA

Received 30 April 2012; revised 17 June 2012; accepted 19 June 2012; published online 9 August 2012.
*For correspondence (e-mail tegeder@wsu.edu).

SUMMARY

Legumes can access atmospheric nitrogen through a symbiotic relationship with nitrogen-fixing bacteroids that reside in root nodules. In soybean, the products of fixation are the ureides allantoin and allantoic acid, which are also the dominant long-distance transport forms of nitrogen from nodules to the shoot. Movement of nitrogen assimilates out of the nodules occurs via the nodule vasculature; however, the molecular mechanisms for ureide export and the importance of nitrogen transport processes for nodule physiology have not been resolved. Here, we demonstrate the function of two soybean proteins – GmUPS1-1 (XP_003516366) and GmUPS1-2 (XP_003518768) – in allantoin and allantoic acid transport out of the nodule. Localization studies revealed the presence of both transporters in the plasma membrane, and expression in nodule cortex cells and vascular endodermis. Functional analysis in soybean showed that repression of *GmUPS1-1* and *GmUPS1-2* in nodules leads to an accumulation of ureides and decreased nitrogen partitioning to roots and shoot. It was further demonstrated that nodule development, nitrogen fixation and nodule metabolism were negatively affected in RNAi *UPS1* plants. Together, we conclude that export of ureides from nodules is mediated by UPS1 proteins, and that activity of the transporters is not only essential for shoot nitrogen supply but also for nodule development and function.

Keywords: allantoin, allantoic acid, legume, nodule development, nitrogen fixation, metabolism, ureide export

INTRODUCTION

Soybean (*Glycine max* L. Merr.) is used as both a food source and a biofuel crop due to its high seed protein and oil levels, and globally its cultivation is exceeded only by wheat and maize (Stacey *et al.*, 2004). Like other legumes, soybean plants are not dependent on nitrogen (N) fertilization for growth due to their ability to form symbioses with atmospheric di-nitrogen (N_2)-fixing bacteroids located in root nodules. While glutamine and asparagine are the main products of N_2 fixation in temperate legumes such as pea and Faba bean, in soybean and *Phaseolus vulgaris* nodules the ureides allantoin and allantoic acid are synthesized. These ureides are the primary transport form of nitrogen from nodules to the shoot (Rainbird, 1982; Smith and Atkins, 2002; Smith *et al.*, 2002; Atkins and Smith, 2007).

For fixation, N_2 enters the bacteroids and is reduced to ammonia by a bacterial nitrogenase. Ammonia (or ammonium) is then released into the cytosol of the infected nodule cell via the peribacteroid membrane, and assimilated to glutamine (Morey *et al.*, 2002; Obermeyer and Tyerman, 2005; Masalkar *et al.*, 2010). In ureide-synthesizing legumes, glutamine moves into both mitochondria and plastids, where it is utilized for *de novo* purine synthesis (Smith and Atkins, 2002). Purines are rapidly degraded to xanthine, which is released to the cytosol and diffuses from infected to uninfected nodule cells. There, xanthine is oxidized in the cytosol to uric acid (Datta *et al.*, 1991), which is then converted in the peroxisomes via the intermediates 5-hydroxyisourate and 2-oxo-4-hydroxy-4-carboxy-5-ureidoimidazoline to allantoin (Hanks *et al.*, 1981; VandenBosch and Newcomb, 1986; Todd *et al.*, 2006; Werner and Witte, 2011). Allantoic acid is produced in the endoplasmic reticulum from allantoin (Werner *et al.*, 2008). Nodule ureide levels are dependent on the legume species (Atkins and Smith, 2007), and reach concentrations of 94 mM in soybean nodule exudate (Streeter, 1979). Following synthesis, the ureides are transported to the nodule vasculature, and leave in the xylem for shoot N supply. More than 80% of the N compounds that exit soybean nodules and that are translo-

cated in the transpiration stream may be in the form of ureides, and the allantoin to allantoic acid ratio may vary from 1:1 to 1:5, depending on the developmental stage of the plant (McClure and Israel, 1979; Streeter, 1979; Schubert, 1981; Rainbird *et al.*, 1984; Gordon *et al.*, 1985).

Soybeans develop spherical, determinate nodules with an inner region that contains the bacteroid-infected cells that function in N_2 fixation and N assimilation, as well as uninfected cells where ureide synthesis occurs. This central zone is surrounded by a layer of inner cortex cells, comprised of the distributing zone and boundary layer, that is bordered by a middle cortex, the sclerid layer, the outer cortex, and finally the periderm (Guinel, 2009). Vascular bundles encircled by an endodermis are located at the periphery adjacent to the inner cortex, and are connected with the root vascular system. Ureide transport within, and export out of, nodules has not been resolved, but may involve a symplasmic and apoplastic route (Brown *et al.*, 1995). In the symplasmic pathway, following synthesis, the ureides travel from the uninfected cells via plasmodesmata to the inner cortex cells, the endodermis and then the nodule vasculature, where they are loaded into the xylem for translocation to the shoot (Selker, 1988; Walsh *et al.*, 1989). Alternatively, ureides are released from the uninfected cells and move via the apoplast to the inner cortex or the vascular endodermis. In soybean, both the Casparian strip of the vascular endodermis (Pate *et al.*, 1969; Walsh *et al.*, 1989) and the boundary layer of the exterior-most inner cortex, where the intercellular wall spaces are occluded by glycoproteins (Parsons and Day, 1990; James *et al.*, 1991; Webb and Sheehy, 1991; Brown and Walsh, 1994), block apoplastic flow of ureides to the xylem (Streeter, 1992). These barriers require uptake of apoplastic ureides into the inner cortex and endodermis cells, respectively, for export from nodules (Brown *et al.*, 1995).

Recently, a French bean (*P. vulgaris* L.) protein called PvUPS1 (ureide permease 1) was identified that mediates transport of allantoin in yeast and is localized in the nodule endodermis (Pélissier *et al.*, 2004). However, the physiological function of UPS1 transporters in legumes, let alone in nodules, has not been demonstrated. In addition, allantoic acid transporters have yet to be identified and characterized *in planta*. UPS transporters have also been found in non-ureide-transporting plant species, specifically AtUPS1–AtUPS5 in Arabidopsis (Desimone *et al.*, 2002; Schmidt *et al.*, 2004, 2006; Froissard *et al.*, 2006). Heterologous expression in yeast and *Xenopus laevis* oocytes demonstrated that AtUPS1, 2 and 5 transport allantoin but have much higher affinities for purines and pyrimidines (e.g. xanthine and uracil), suggesting that compounds structurally related to allantoin represent the physiological substrates of UPS transporters in Arabidopsis.

The present work addresses the role of soybean UPS1 transporters in export of ureides from the nodules, and their significance in nodule physiology and development. We first describe the functional characterization of ureide permeases GmUPS1-1 and GmUPS1-2 in yeast, supporting a role for UPS1 proteins in allantoin as well as allantoic acid transport. Using cellular and subcellular localization studies, we then demonstrate that GmUPS1-1 and 1-2 are plasma membrane proteins that are expressed in the nodule inner cortex and vascular endodermis, suggesting a role in export of both allantoin and allantoic acid from the nodule. This is confirmed by phenotypic, molecular and biochemical analyses of composite soybean plants with silenced *GmUPS1* expression in nodules. Supported by molecular, structural and physiological studies, it is further demonstrated that ureide transport processes are important for nodule development, and influence atmospheric N_2 fixation and N assimilation. Finally, the function of the two ureide transporters in N transfer from nodules to shoot is discussed, and their importance for nodule function is evaluated.

RESULTS

GmUPS1-1 and GmUPS1-2 function in ureide import into the soybean cells

Using an RT-PCR approach and primers designed along soybean homologs of *PvUPS1* (Pélissier *et al.*, 2004), we isolated two *UPS1* cDNAs from soybean nodules that share 98 and 96% similarity at the nucleotide and amino acid level, respectively. The putative ureide transporter genes were named *GmUPS1-1* (Glyma01g07120) and *GmUPS1-2* (Glyma02g12970).

To determine whether the GmUPS1 proteins are functional transporters, direct uptake studies using [^{14}C]allantoin were performed using an allantoin transport-deficient yeast mutant expressing either *GmUPS1-1* or *GmUPS1-2.* Both GmUPS1 transporters mediated uptake of allantoin into yeast cells and exhibited classical Michaelis–Menten saturation kinetics with K_m values of 76 and 54 μM, respectively (Figure 1a,b).

To examine whether the soybean UPS1 proteins transport allantoic acid and other substrates of the purine synthesis or salvage pathway in addition to allantoin, competition experiments measuring [^{14}C]allantoin uptake in the presence of a 10-fold molar excess of non-radioactive competitors were performed (Figure 1c). The results show that xanthine and uracil are strong competitors for allantoin uptake into yeast, similar to what was shown for French bean and Arabidopsis UPSs (Desimone *et al.*, 2002; Pélissier *et al.*, 2004; Schmidt *et al.*, 2004, 2006). However, while the allantoin and allantoic acid levels in nodules are high, in comparison the xanthine and uracil concentrations are negligible (Fujihara and Yamaguchi, 1978), and therefore they are most probably not substrates for the GmUPS1 transporters under physiological conditions. In contrast to previous studies, here we found that allantoic acid also

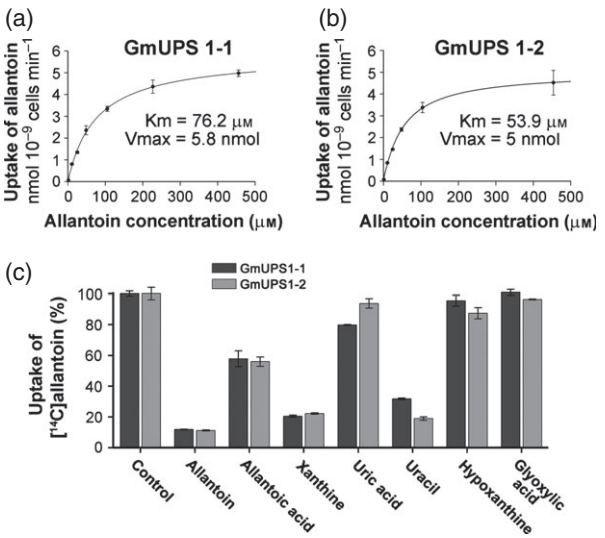

Figure 1. Functional characterization of GmUPS1-1 and GmUPS1-2 in yeast.
(a, b) [^{14}C]allantoin uptake in *dal4/dal5* cells expressing *GmUPS1-1* (a) or *GmUPS1-2* (b). The GmUPS1 proteins display Michaelis–Menten kinetics, with K_m values in the 53-77 μM range. Values are means ± SD of four independent experiments.
(c) Substrate specificity of *GmUPS1-1* or *GmUPS1-2*. Competition for [^{14}C]allantoin uptake into *dal4*/*dal5* cells in the presence of a 10-fold excess of allantoic acid, purines, purine degradation products or allantoin (positive control) or without competitors (negative control). Values are means ± SD of four independent experiments.

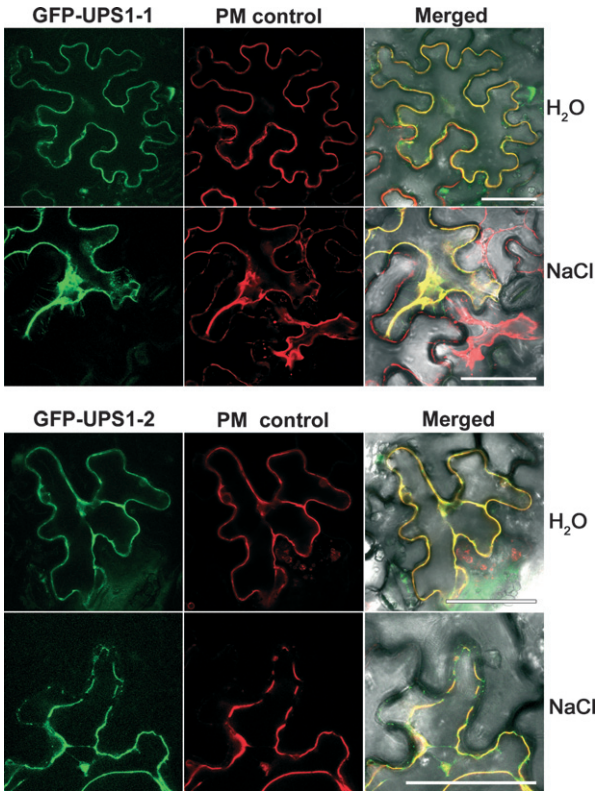

Figure 2. Subcellular localization of GmUPS1-1 and GmUPS1-2.
GFP–GmUPS1-1 and GFP–GmUPS1-2 fusion proteins were transiently expressed in *Nicotiana benthamiana* leaves using an *Agrobacterium* infiltration method (left column). *Arabidopsis thaliana* aquaporin AtPIP2A fused to mCherry was used as control for plasma membrane localization (middle column). The right column shows merged images for GmUPS1 and AtPIP2A proteins. Some cells were plasmolyzed (NaCl, plasmolyzed; H_2O, non-plasmolyzed) to visualize plasma membrane localization more clearly. Scale bars = 50 μm.

competed with allantoin uptake, indicating that GmUPS1-1 and GmUPS1-2 transport allantoic acid as well (Figure 1c). However, it may also be possible that allantoic acid partially inhibits the transport of allantoin without being transported itself.

The subcellular localization of UPS proteins is unknown, and to analyze whether the GmUPS1 proteins are functioning in cellular import or transport across subcellular membranes, GFP–GmUPS1-1 and GFP–GmUPS1-2 fusion proteins were localized in *Nicotiana benthamiana* leaf cells. Using confocal laser scanning microscopy, it was demonstrated that both GmUPS1-1 and GmUPS1-2 are targeted to the plasma membrane, which was even more evident when the leaves were plasmolyzed (Figure 2). Together, the results suggest a role for GmUPS1 proteins in cellular uptake of apoplastic allantoin and allantoic acid.

UPS1 transporters are expressed in the nodule cortex and vascular endodermis

To determine whether there are differences in the location of function between *GmUPS1-1* and *GmUPS1-2* in soybean nodules, RNA localization studies were performed. The *in situ* RT-PCR method was used, as, in contrast to the conventional RNA hybridization procedure, it allows specific amplification of highly similar genes and has fewer problems with background staining (Lee and Tegeder, 2004). Taken together, our results differ from previous studies with French bean *PvUPS1.* In addition to expression in the endodermis and vascular bundles (Pélissier *et al.*, 2004), both *GmUPS1-1* and *GmUPS1-2* were also expressed in the inner cortex (Figure 3a–f), suggesting a role for GmUPS1-1 and GmUPS1-2 in allantoin and allantoic acid uptake along the route from uninfected nodule cells to the vasculature. Some *GmUPS1-1* and *GmUPS1-2* expression was also found in the outer cortex as well as in the sclerid layer. In these cells, the GmUPS1 transporters may function in retrieval of ureides from the apoplast to prevent leakage into the soil and to redirect them in the symplast to the vasculature.

In previous studies, we isolated the *PvUPS1* promoter from French bean (1255 bp, Figure S1), and we used this to create a *PvUPS1* promoter–*GUS* construct in nodulated composite soybean plants to test whether the promoter targets gene expression in nodules to the same cell types in which the *GmUPS1* transporters are expressed (Figure 3a–d) and to determine whether this promoter could be used

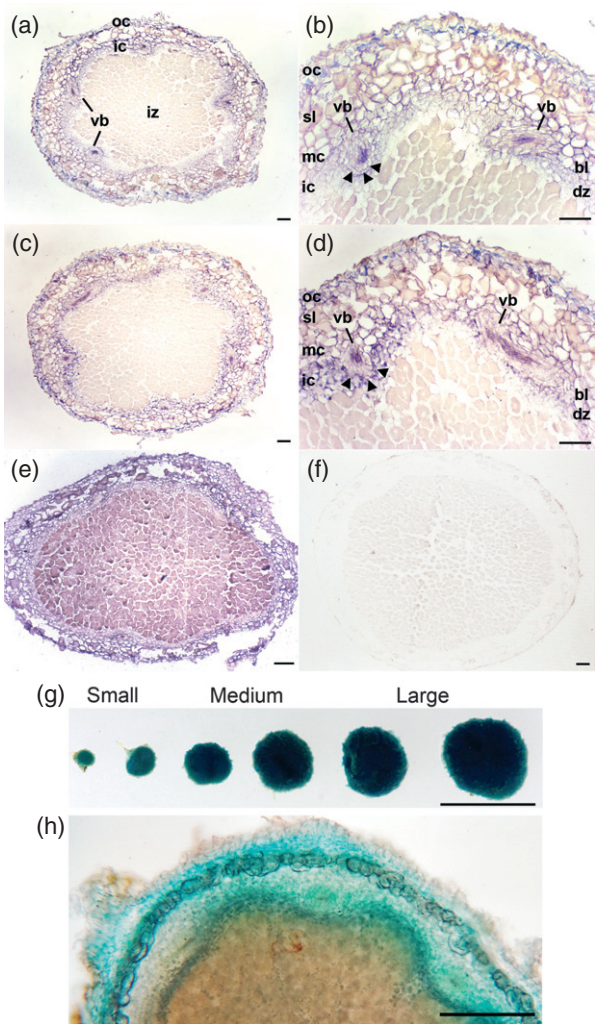

Figure 3. *UPS1* localization in soybean nodules.
(a–f) *In situ* RT-PCR. Nodule RNA was reverse-transcribed and specific cDNAs were amplified directly on nodule tissue sections and color detection method was used to visualize the location of the specific transcripts (Lee and Tegeder, 2004). bl, boundary layer; iz, infected zone; ic, inner cortex; mc, middle cortex; oc, outer cortex; vb, vascular bundles; sl, sclerid layer; dz, distributing zone. Arrow heads in (b) and (d) point to the vascular endodermis. Scale bars = 50 μm. (a, b) Localization of *GmUPS1-1*. (c, d) Localization of *GmUPS1-2*.
(e) 18S rRNA amplification (positive control).
(f) PCR reaction performed without primers (negative control).
(g, h) *PvUPS1* promoter–*GUS* studies. (g) GUS expression throughout nodule development. For biochemical, structural and molecular analyses (see Figures 4, 5 and 7), nodules were grouped by size: small (<3.5 mm^2), medium (3.5–4.5 mm^2) and large (>4.5 mm^2). Scale bar = 5 mm. (h) Light micrograph of a cross-section of a transgenic GUS-stained nodule. Scale bar = 250 μm.

for an *UPS1* silencing approach in nodules (see below). Developing transgenic hairy roots were infected with *Bradyrhizobium japonicum* to induce production of transgenic nodules. The nodules were analyzed using GUS assays, and the results showed staining throughout nodule development (Figure 3g). GUS staining was specifically found in the nodule cortex and vasculature and the vascular endodermis (Figure 3h), consistent with the localization of *GmUPS1-1* and *GmUPS1-2* in nodules (Figure 3a–h). These results demonstrate that the *PvUPS1* promoter is well suited to silence *GmUPS1* expression in nodules (see below).

Repression of *UPS1* expression in nodules causes reduced nodule development

To determine the physiological function of the GmUPS1 transporters in nodules, we silenced *GmPS1-1* and *GmUPS1-2* expression using composite soybean plants, a strategy that has been successfully applied in recalcitrant soybean to analyze gene function in nodules or roots (Subramanian *et al.*, 2004, 2006; Collier *et al.*, 2005; Libault *et al.*, 2009). In *ex vitro* composite legumes, transgenic nodulated roots can be produced in combination with a non-transgenic shoot (Collier *et al.*, 2005). For targeted *GmUPS1* repression, both *GmUPS1-1* and *GmUPS1-2* were concurrently repressed in soybean nodules using an RNAi approach under the control of the *PvUPS1* promoter (Figures 3g,h and 4, and Figure S1). Composite plants expressing RNAi *GFP* were used as controls to ensure that potential changes in RNAi *UPS1* nodules were not due to alterations in gene expression caused by induction of the RNAi machinery (Figure 4). When analyzing the transgenic nodules, an obvious difference in nodule development was observed (Figure 4a–d). Although the total number of nodules was unchanged in RNAi *UPS1* plants (Figure 4e), the number of medium-sized (1.59–1.98 mm diameter) and large (>1.98 mm) nodules was significantly decreased by 60% compared to the RNAi control, and the amount of small nodules (<1.59 mm) was increased by 51% (Figure 4f), suggesting an arrest in development of RNAi *UPS1* nodules.

UPS1 expression experiments were performed using RNA from medium-sized nodules to analyze whether the observed nodule phenotype coincides with decreased levels of *GmUPS1* transcripts. The results showed 50 and 80% reductions in *GmUPS1-1* and *GmUPS1-2* expression, respectively (Figure 4g).

Repression of *UPS1* expression leads to increased ureide levels in nodules and affects N translocation from nodule to shoot

Cellular and subcellular localization as well as the biochemical analyses in yeast suggest that both GmUPS1-1 and GmUPS1-2 import allantoin and allantoic acid into inner cortex and endodermis cells for export from the nodules and translocation to the shoot. To further resolve UPS1 function *in planta*, ureide levels were determined in RNAi *UPS1* nodules of various sizes (Figure 5). Ureide levels were significantly increased in all nodules by 20–116%, with the highest increase occurring in large nodules (Figure 5a–c). In general, the ureides comprised approximately 30% allantoin and 70% allantoic acid. The elevation in total ureides was

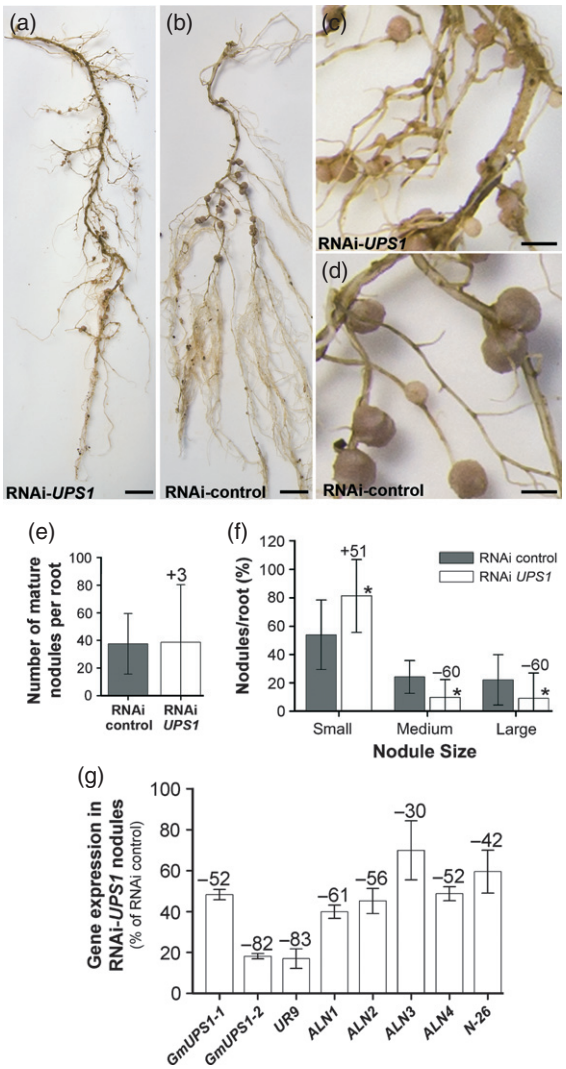

Figure 4. Analyses of nodule development and gene expression in RNAi *UPS1* nodules.
(a, c) Nodulated RNAi *UPS1* roots. Scale bars = 1 cm (a) and 2 mm (c).
(b, d) Nodulated RNAi control roots. Scale bars = 1 cm (b) and 2 mm (d).
(e) Total nodule number in RNAi plants.
(f) Development of small, medium and large transgenic nodules on roots of RNAi *UPS1* and RNAi control plants.
For (e) and (f), transgenic nodules were derived from 16 RNAi *UPS1* and RNAi control plants, respectively. The results are representative of at least two independent experiments. Error bars show standard deviation. One-way analysis of variance (ANOVA) was used to determine statistical significance. Asterisks indicate significant differences from the RNAi control nodules ($P < 0.001$). Values above the columns indicate the percentage change compared to RNAi controls.
(g) Real-time PCR analysis of *GmUPS1* transporters and genes involved in nitrogen export from symbiosomes and in nodule ureide synthesis. RNA from medium-sized nodules was used. Expression of the ureide transporter genes *GmUPS1-1* (Glyma01g07120) and *GmUPS1-2* (Glyma02g12970), and genes encoding Nod26 involved in ammonium translocation across the peribacteroid membrane (*N-26*), nodule uricase Nod35 (*Ur9*) and allantoinases ALN1–4 (*ALN1*–*ALN4*) were analyzed. The expression levels were measured from three technical replicates relative to soybean miR156a, mi156b or miR1520d used as control genes (Kulcheski *et al.*, 2010). Shown is the percent change in gene expression relative to miR1520d expression, determined from the C_T values by using the $2^{-\Delta\Delta C_T}$ method (Livak and Schmittgen, 2001).

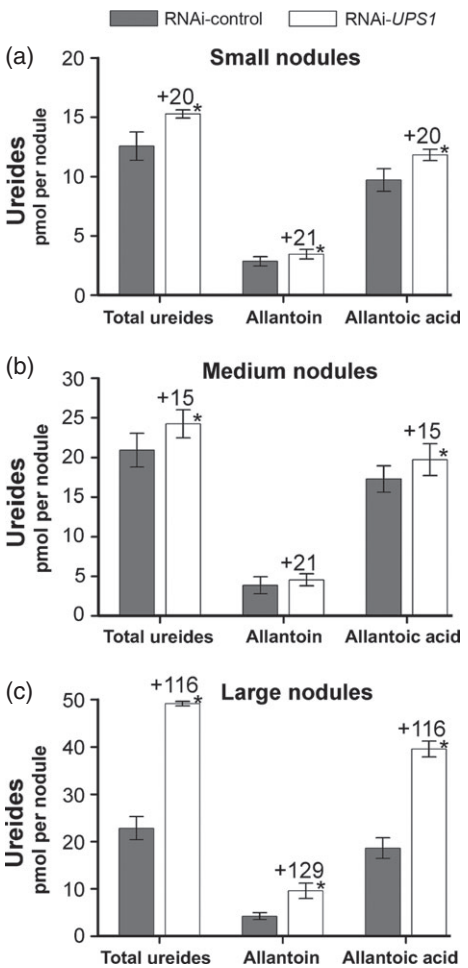

Figure 5. Total ureides, and allantoin and allantoic acid concentrations in RNAi *UPS1* nodules.
(a) Small nodules (<3.5 mm^2).
(b) Medium nodules (3.5–4.5 mm^2).
(c) Large nodules (>4.5 mm^2).
The results are representative of at least two independent experiments. Measurements are from three pools of nodules, each derived from at least two roots of six plants. Error bars show standard deviation, and asterisks indicate significant differences from the RNAi control ($P < 0.02$). Values above the columns indicate the percentage change compared to RNAi controls.

due to an increase in both allantoin and allantoic acid, supporting a role for GmUPS1-1 and GmUPS1-2 in export of the two ureides from the nodule.

Ureides leave the nodule via the xylem that is connected to the root vasculature. Levels of ureides in RNAi *UPS1* roots and xylem were examined to analyze whether N transport from nodules to roots and finally the shoot was altered. Allantoin and allantoic acid contributed approximately 30 and 70%, respectively, of the total ureide levels in both roots and xylem sap (Figure 6a,b). A significant decrease in allantoin as well as allantoic acid levels was detected in RNAi *UPS1* roots compared to the RNAi control roots, leading to an overall reduction in total ureide

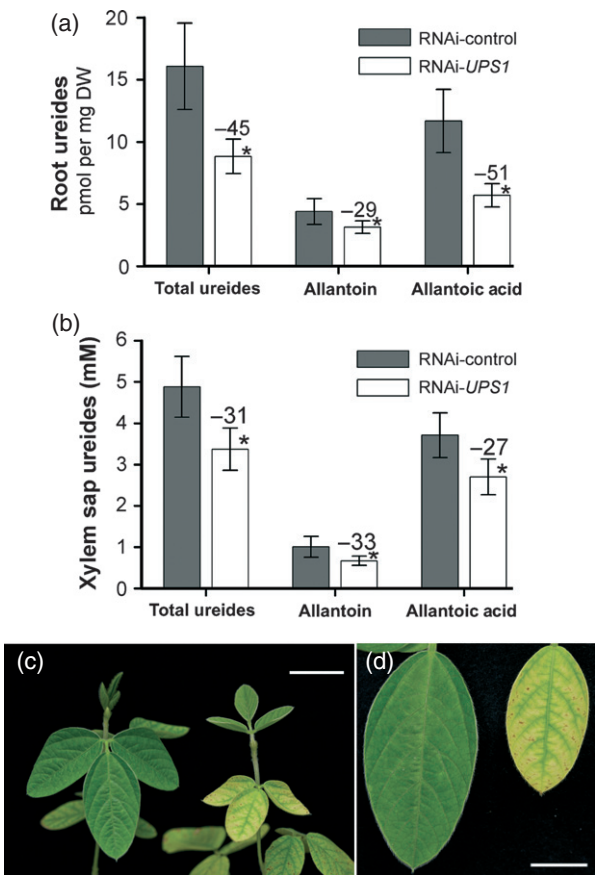

Figure 6. Ureide levels in roots and xylem sap, and shoot phenotype of RNAi *UPS1* composite plants.
(a) Total ureides, and allantoin and allantoic acid levels in roots.
(b) Total ureides, and allantoin and allantoic acid levels in xylem sap.
The results are representative of at least two independent experiments. Root ureide measurements are from three pools of roots, each pool derived from at least two roots of six plants. Xylem sap was collected from eight individual plants. Error bars show standard deviation. Asterisks indicate significant differences from the RNAi control ($P < 0.02$). Values above the columns indicate the percentage change compared to RNAi controls.
(c, d) Leaves of composite RNAi control plants (left) and RNAi *UPS1* (right) grown for 6 weeks in nitrogen-free Turface medium. Roots were inoculated with *Bradyrhizobium japonicum* and developed nitrogen-fixing nodules. Scale bars = 2 cm (c) and 1 cm (d).

amounts of 45% (Figure 6a). In addition, ureide levels (i.e. allantoin and allantoic acid) in the xylem sap of RNAi *UPS1* composite plants were significantly decreased by 31% compared to control plants (Figure 6b), further confirming that nodule to root to shoot translocation of ureides was altered due to *UPS1* repression in nodules. A decrease in N partitioning from nodule to shoot was also evident when analyzing the shoot phenotype of the composite plants. It was found that the leaf size was reduced in RNAi *UPS1* shoots, and the intercostal fields of leaves were yellowish while the leaf veins were green, which is consistent with N deficiency symptoms (Figure 6c,d).

UPS1 expression affects nodule metabolism and N_2 fixation

Using quantitative PCR, we further determined whether *UPS1* repression and subsequent accumulation of ureides in nodules affect the expression of genes involved in ureide synthesis (Figure 4g). Transcript levels of *UR9* encoding the root-specific Nod 35 uricase involved in synthesis of allantoin precursor 5-hydroxyisourate (Bergmann *et al.*, 1983; Kahn *et al.*, 1997; Takane *et al.* 1997), and of *ALN1–ALN4* (Glyma15g07910, Glyma13g31430, Glyma15g07920 and Glyma13g31420; Duran and Todd, 2012) encoding allantoinases responsible for conversion of allantoin to allantoic acid, were analyzed. Expression of *UR9* was decreased by 83% in RNAi *UPS1* nodules, and transcript levels of *ALN1–ALN4* were reduced by between 30 and 61% (Figure 4g). These results suggest that elevated nodule ureide levels down-regulate allantoin and allantoic acid synthesis at the transcriptional level.

Expression of *N-26* encoding Nod 26, which is involved in ammonium/ammonia transport from the bacteroid-containing symbiosomes to the infected nodule cells (Fortin *et al.*, 1987; Masalkar *et al.*, 2010), was analyzed. The level of *N-26* transcripts was reduced, suggesting a decrease in N delivery from the bacteroids to the plant cells (Figure 4g). To resolve whether atmospheric N_2 fixation by the bacteroids was also affected, an acetylene reduction assay was performed with small, medium and large nodules. The results demonstrate that N_2 fixation was decreased in all RNAi *UPS1* nodules by 32-44% (Figure 7a).

Using light microscopy, it was then determined whether the reduction in N_2 fixation was due to changes in the structure of RNAi *UPS1* nodules. We compared small, medium and large nodules of RNAi *UPS1* and RNAi control plants and obtained similar results. As shown in Figure 7(b) for medium-sized nodules, the infected cells in all RNAi *UPS1* nodules analyzed were generally smaller compared to control nodules. This suggests that infected cells in RNAi *UPS1* nodules failed to increase in size as the nodule matured, probably due to ureide-induced altered bacteria infection, bacteroid development or endo-reduplication of the infected cells (James *et al.*, 1991; Maunoury *et al.*, 2008; Libault *et al.*, 2011).

DISCUSSION

Soybean UPS1 proteins mediate transport of allantoin and allantoic acid

Nodulated legumes such as soybean and French bean use ureides as the main long-distance transport form of nitrogen, and plasma membrane transporters have been hypothesized to be required for partitioning of allantoin and allantoic acid from nodules to shoot (Pélissier *et al.*, 2004). Recent transport studies with yeast and *Xenopus* oocytes expressing *UPS* transporters from Arabidopsis and French

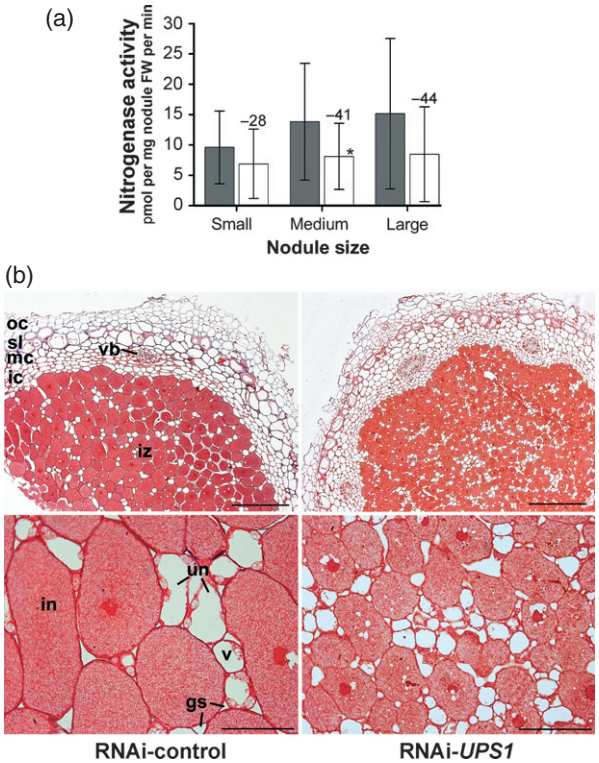

Figure 7. Analysis of N_2 fixation rate and morphology of RNAi *UPS1* nodules.
(a) Atmospheric N_2 fixation in small, medium and large RNAi *UPS1* nodules. Nitrogenase activity was determined using the acetylene reduction assay. A total of 30 measurements were taken for each nodule size from at least 15 plants. The results are representative of at least two independent experiments. Error bars show standard deviation, and asterisks indicate significant differences for RNAi *UPS1* nodules compared to the RNAi control ($P < 0.02$). Values above the columns indicate the percentage change compared to RNAi controls.
(b) Light micrographs of RNAi nodule cross-sections stained with safranin. Compared to RNAi control nodules (left column), infected cells of RNAi *UPS1* nodules are generally smaller (right column). The results shown are for medium-sized nodules but are also representative of small and large nodules. in, infected cell; iz, infected zone; ic, inner cortex; mc, middle cortex; oc, outer cortex; sl, sclerid layer; un, uninfected cell; vb, vascular bundles; v, vacuole; gs, gas space. Scale bars = 50 μm (upper images) and 250 μm (lower images).

bean demonstrated that UPS proteins mediate transport of allantoin and other heterocyclic products of the purine synthesis and degradation pathway with varying substrate affinity. However, the UPS proteins were not involved in allantoic acid transport (Desimone *et al.*, 2002; Pélissier *et al.*, 2004; Schmidt *et al.*, 2004, 2006; Pélissier and Tegeder, 2007), and their physiological function remained unresolved. The results presented here suggest that soybean UPS1 proteins transport both allantoin and allantoic acid. This is supported by yeast transport studies (Figure 1) as well as biochemical analyses of RNAi *UPS1* soybean plants showing an accumulation of allantoin and allantoic acid in nodules and a decrease of these ureides in roots and xylem sap when *GmUPS1-1* and *GmUPS1-2* expression in nodules is repressed (Figures 5 and 6a,b). We have no clear explanation why, in contrast to the GmUPS1 proteins, PvUPS1 does not transport or mediate the uptake of allantoic acid (Pélissier *et al.*, 2004), although it is present in relatively high amounts in French bean nodules (Alamillo *et al.*, 2010). However, PvUPS1 function was only analyzed in yeast, and future *in planta* studies may resolve the complete substrate spectrum of the PvUPS1 transporter. In addition, as in soybean, French beans may have two UPS1 proteins, and there may be some variation in substrate specificity between these proteins. In soybean, *GmUPS1-1* and *GmUPS1-2* appear to be the product of gene duplication (Schmutz *et al.*, 2010), and our data show that they have similar substrate specificity, localization and function in plants.

GmUPS1 function is essential for ureide export from nodules and for shoot N supply

Soybeans produce determinate nodules with a center comprising infected and uninfected cells. This central tissue is surrounded by an inner, middle and outer cortex ensconced with the vascular system that allows import of shoot/phloem-derived metabolites and export of the ureides from the nodules via the xylem (Selker, 1988). Symplasmic movement of the ureides out of the nodules is generally possible as plasmodesmata connect the various nodule cells, creating a symplasmic continuum from the uninfected cells to the vascular pericycle cells (Selker and Newcomb, 1985; Selker, 1988; Brown *et al.*, 1995). However, the frequency of plasmodesmata varies between the cell types and appears to be relatively low between the inner cortex and vascular endodermis, and it has been suggested that the plasmodesmata may be involved in entry of large amounts of shoot/phloem-derived sucrose and other metabolites to the infected cells for N_2 fixation (Brown *et al.*, 1995). Metabolite analyses of the cortical apoplast showing significant levels of ureides and low amounts of sucrose confirm that sucrose moves symplasmically into the infected nodule zone while ureides are transported apoplastically to the vasculature (Walsh *et al.*, 1989; Streeter, 1992; Streeter and Salminen, 1993; Brown *et al.*, 1995). Nevertheless, when the ureides reach the Casparian strip of the vascular endodermis (Pate *et al.*, 1969; Walsh *et al.*, 1989), plasma membrane transporters are required for their import into the symplasm to bypass the cell-wall blockade (Pélissier *et al.*, 2004). In addition, apoplastic flow may be blocked in the inner cortex by the boundary layer, where intercellular wall spaces contain glycoprotein occlusions, requiring import of ureides into the cortex cells (Newcomb *et al.*, 1989; Parsons and Day, 1990; James *et al.*, 1991; Webb and Sheehy, 1991; Streeter, 1992). Localization of GmUPS1-1 and GmUPS1-2 in the plasma membrane and to the inner cortex and vascular endodermis, as well as their functional analysis in yeast, support the existence of an apoplastic transport mechanism for ureides within the nodules, and the function of both GmUPS1-1 and GmUPS1-2 in uptake of allantoin and allan-

toic acid into the symplasm for export out of the nodule and N shoot supply. This is further supported by functional analyses of the GmUPS1 transporters using RNAi *UPS1* soybean plants, showing an accumulation of allantoin and allantoic acid in nodules, a decrease of the ureides in roots and xylem sap, and N deficiency symptoms in leaves (Figures 5 and 6).

GmUPS1 function is important for nodule metabolism and nitrogen fixation

Inhibition of N_2 fixation has been studied extensively, and it has been suggested that ureide accumulation in soybean shoots (de Silva *et al.*, 1996; Serraj *et al.*, 1999b; Vadez and Sinclair, 2001) and in nodules (Vadez *et al.*, 2000; de Beer *et al.*, 2007; van Heerden *et al.*, 2008; Vauclare *et al.*, 2010) under drought or cold stress down-regulates nodule nitrogenase activity. This regulation of N_2 fixation may occur via feedback inhibition induced by elevated N amounts in the leaves, or it may be directly controlled by high ureide levels (or related N compounds) in the nodules (Sinclair and Serraj, 1995; Serraj *et al.*, 1999b, 2001; Vadez and Sinclair, 2000, 2001). Recent work with drought-stressed soybean nodules suggests that a local rather than a systemic N signal regulates nitrogenase activity (King and Purcell, 2005; Ladrera *et al.*, 2007). Our studies showing increased allantoin and allantoic acid levels in RNAi *UPS1* nodules and a concurrent decrease in N_2 fixation are in agreement with this (Figures 5 and 7a). Further, our results confirm previous predictions that the observed ureide accumulation in nodules and the subsequent effects on nodule activity are due to altered ureide export (Streeter, 1993, 2003; Walsh, 1995; Serraj *et al.*, 1999a). Elevated levels of N_2 fixation products also appear to feedback-regulate N delivery from the symbiosome and N metabolism in nodules, as indicated by decreased transcript levels of *UR9* and ureide synthesis genes (Figure 4g), corroborating the previously described regulation of primary nodule metabolism under drought (and high nodule N) conditions (Larrainzar *et al.*, 2007).

GmUPS1 is critical for nodule development

Generally, successful nodulation and nodule development occurs under N-limiting conditions, and it is widely accepted that high N levels in the soil inhibit legume nodulation (Herridge *et al.*, 1984) and nodule development (Imsande, 1986), in addition to their detrimental effect on nitrogenase activity (Purcell and Sinclair, 1990). In our studies, the number of nodules was not changed in RNAi *UPS1* plants, but nodule development was inhibited (Figure 4a–f). In addition, independent of the nodule size, the infected cells were generally smaller in RNAi *UPS1* plants compared to the control plants (Figure 7b), probably due to differences in bacteria infection, bacteroid development or endo-reduplication of the infected cells (Parsons and Day, 1990; James *et al.*, 1991; Maunoury *et al.*, 2008; Libault *et al.*, 2011). Together, the results demonstrate that N transporter activity in nodules is not only essential for N export from the nodule, but also for regulating nodule N levels affecting nodule size, as well as the development and function of bacteroid-containing infected cells. They further indicate that a signal downstream of nodule initiation causes the observed alteration, and that the signal is nodule-localized rather than systemic (Eaglesham, 1989; Abaidoo *et al.*, 1990). The high levels of ureides or related N compounds in RNAi *UPS1* nodules may induce the developmental changes, as a similar effect was observed when nodules were supplied with nitrate, and nodule maturation resumed upon removal of N (Fujikake *et al.*, 2003). However, inter-related metabolic pathways such as carbon metabolism are most probably also altered in RNAi *UPS1* nodules, and may lead to the arrest in nodule growth (Parsons and Day, 1990; James *et al.*, 1991; Green and Emerich, 1997; Van Dao *et al.*, 2008; Libault *et al.*, 2011). Future transcriptome and metabolome analyses may help to identify the signals as well as resolve further interactions between N transport and nodule physiology.

PERSPECTIVES

This work demonstrates that UPS1 transporters are important for the export of allantoin and allantoic acid out of the nodules. Our results further suggest that ureide transporters control nodule allantoin and allantoic acid levels, and that these ureides or related N compounds provide regulatory signals for atmospheric N_2 fixation and nodule metabolism, growth and potentially rhizobia infection. Investigations are now required to establish how nodule ureide transporters are controlled, and if and how allantoin or allantoic acid act as a signaling molecule for nodule function and development. We also intend to address whether increased ureide export positively affects N_2 fixation and N shoot supply in stressed environments (i.e. drought and cold) and non-stressed environments, with beneficial consequences for plant performance and seed yield.

EXPERIMENTAL PROCEDURES

Materials and growth conditions

Plants of *Glycine max* cultivar Hutcheson (Buss *et al.*, 1988) were grown in the growth chamber under a 16 h photoperiod and light intensity of 1000 μmol photons m^{-2} sec^{-1}. The day/night temperature and relative humidity were 26°C/21°C and 50%/70%, respectively. For DNA or RNA expression analyses, soybean plants were grown in Turface MVP Infield Conditioner (Hummert, http://www.invitrogen.com/) in 4 L pots. The seeds were inoculated with *Bradyrhizobium japonicum* strain USDA110. Plants were watered twice per day (approximately 1 L each time), and fertilized every 2 days using an N-free plant nutrient solution (Lullien *et al.*, 1987). The production of nodulated composite soybean plants and their growth media is explained below. French bean (*Phaseolus vulgaris* cv. Redland) plants were grown in the greenhouse as previously described (Pélissier *et al.*, 2004).

Isolation of soybean *UPS1* transporters

To isolate the soybean *UPS1* transporters, primers (Table S1) were designed based on the *PvUPS1* homologs Glyma01g07120 (*GmUPS1-1*) and Glyma02g12970 (GmUPS1-2) [http://www.phytozome.net or the National Center of Biotechnology Information database (http://www.ncbi.nlm.nih.gov/); accessions XP_003516366 and XP_003518768, respectively]. Nodule cDNA was synthesized as previously described (Collier *et al.*, 2005), and PCR was performed using Platinum® *Taq* high-fidelity DNA polymerase (Invitrogen, http://www.invitrogen.com/). PCR products were cloned into pGEM®-T-Easy (Promega, http://www.promega.com/) and sequenced.

Isolation of the *PvUPS1* promoter

For promoter isolation, genomic DNA of *P. vulgaris* was digested with *Eco*47I, self-ligated with T4 DNA ligase (Fermentas/, http://www.fermentas.com/), and used as template for inverse PCR with opposed primers designed to the 5′ end of *PvUPS1* cDNA (Table S1). The resulting 1518 bp PCR product was cloned into pGEM®-T-Easy and sequenced. The promoter sequence upstream of the *PvUPS1* ATG was then amplified by PCR using promoter primers tailed with 5′ *Hin*dIII and 3′ *Eco*RI (Table S1), cloned into pGEM®-T-Easy and sequenced. The final 1255 bp promoter sequence was analyzed for regulatory motifs using the Plant *Cis*-Acting Element Database (PLACE) (Higo *et al.*, 1998). Putative regulatory elements and references are shown in Figure S1.

Biochemical characterization of GmUPS1-1 and GmUPS1-2 in yeast

GmUPS1-1 and *GmUPS1-2* cDNAs were transferred from pGEM®-T-Easy into the *Eco*RI site of yeast expression vector pDR196 (Rentsch *et al.*, 1995). Yeast strain *dal4*/*dal5*, which is deficient in allantoin transport (Desimone *et al.*, 2002), was transformed with *GmUPS1-1* or *GmUPS1-2*/pDR196 as described by Dohmen *et al.* (1991), and growth complementation studies were performed on medium containing allantoin as sole nitrogen source. *PvUPS1*/pDR196 (Pélissier *et al.*, 2004) and the empty vector were used as controls. Direct uptake studies using [7-^{14}C]-labeled allantoin as well as competition studies to determine the substrate specificity of GmUPS1-1 and GmUPS1-2 were performed as previously described (Pélissier *et al.*, 2004). Allantoin, allantoic acid and other substrates of the purine synthesis or salvage pathway including xanthine, uric acid, uracil, hypoxanthine and glyoxylic acid were used as competitors and supplied in 10-fold excess.

Construct preparation for plant transformation

For construct preparation, vectors from the Modular Binary Construct System (MBCS, Collier *et al.*, 2005) kindly provided by Dr Christopher Taylor (Department of Plant Pathology, Ohio State University, Wooster, OH, USA) were used. These vectors are modified pBluescript IIKS+ vectors containing a variety of promoters/genes and either a *Super Ubiquitin* (*SU*) intron (Perera and Rice, 2002) or the *Flaveria trinervia* pyruvate orthophosphate dikinase intron from pKANNIBAL (Helliwell *et al.*, 2002). To prepare the *PvUPS1* promoter–*GUS* construct, the *PvUPS1* promoter was cloned using *Hind*III/*Eco*RI into an MBCS plasmid containing an *SU* intron followed by a nuclear localization signal (*NLS*) (Raikhel, 1992), the *uidA* gene (*GUS*) encoding β-glucuronidase (Jefferson *et al.*, 1987), and the nopaline synthase (*NOS*) terminator (Bevan *et al.*, 1983).

For subcellular localization, *UPS1* transporters–*GFP* gene fusion constructs were prepared using an MBCS vector containing the *SU* promoter, the *SU* intron and a full-length *GFP5* gene (Siemering *et al.*, 1996). The *Pac*I restriction sites were substituted by *Sda*I sites, and the *GFP* gene was replaced with either *GmUPS1-1* or *GmUPS1-2* (*Bam*HI/*Sac*I). An adapter (Table S1) was added using *Bam*HI/*Bgl*II upstream of the *UPS1* cDNAs. A *GFP5* gene without a stop codon was cloned into the *Bam*HI site upstream of the adapter, resulting in a final cassette comprising *SU* promoter–*SU* intron–*GFP*–adapter–*GmUPS1-1/GmUPS1-2*–NOS terminator.

To prepare an RNAi-*UPS1* construct, an MBCS vector containing the figwort mosaic virus (*FMV*) promoter, *Kannibal* intron (Helliwell *et al.*, 2002) and octopine synthase terminator (*OCS*) was used. First, the *FMV* promoter was replaced using *Sac*I/*Kpn*I by a *PvUPS1* promoter PCR product tailed with *Sac*I/*Kpn*I sites. An adapter containing *Nde*I and *Sal*I restriction sites (see Table S1) was then cloned using *Kpn*I downstream of the *PvUPS1* promoter. To simultaneously silence both *GmUPS1* transporters in nodules, a PCR fragment was produced along a conserved region of *GmUPS1-1* and *GmUPS1-2* (positions 31–562) and restriction sites were added (5′, *Xba*I and *Nde*I; 3′, *Sal*I and *Xba*I; see Table S1 for primers). The *GmUPS1* silencer fragments were cloned using *Nde*I/*Sal*I (sense) upstream of the *Kannibal* intron, and using *Xba*I (antisense) downstream of the intron, resulting in a final cassette comprising *PvUPS1* promoter–*UPS1* silencer (sense)–adapter–*Kannibal* intron–*UPS1* silencer (antisense)–*OCS* terminator. To ensure that any phenotype observed in RNAi *UPS1* plants is based on *UPS1* repression and not an RNAi effect, a control vector was produced containing an exogenous (non-plant) gene, i.e. *GFP*. RNAi *GFP* constructs were created by cloning *GFP* silencer fragments (717 bp, see Table S1 for primers) instead of *UPS1* silencers up stream and downstream of the *Kannibal* intron (*Kpn*I, sense; *Bam*HI/*Hind*III, antisense).

Depending on the construct (see above), the prepared cassettes were removed from the shuttle vectors using either *Pac*I or *Sda*I, and transferred into the MBCS binary plasmid, which is a modified pBIN19 vector (Collier *et al.*, 2005). The modified pBIN19 used for the RNAi constructs additionally contained an *SU* promoter–*GUS*–*NOS* terminator cassette on the T-DNA that allows visual identification of successful transformation of nodulated roots in composite plants using the GUS assay (see below). The binary vectors harboring the *SU* promoter–*GFP*–*GmUPS1-1* or *SU* promoter–*GFP*–*GmUPS1-2* constructs were transferred into *Agrobacterium rhizogenes* 18r12v (Veena and Taylor, 2007), a disarmed variant of strain NCPPB2659 (Combard *et al.*, 1987), using electroporation (McCormac *et al.*, 1998). Binary vectors containing the *PvUPS1* promoter–*GUS* and the *PvUPS1* promoter–RNAi *UPS1* or RNAi *GFP* (control) constructs were transferred into strain NCPPB2659, that induces the development of (transgenic) hairy roots (Combard *et al.*, 1987).

Subcellular localization of GmUPS1 proteins

For subcellular localization of *GFP*–*GmUPS1-1* or *GFP*–*GmUPS1-2* fusions, the *Nicotiana benthamiana* Domin leaf infiltration method was used (Sparkes *et al.*, 2006). *Agrobacterium rhizogenes* 18r12v carrying *GFP*–*GmUPS1* transporter fusion protein constructs was co-infiltrated with *A. tumefaciens* strain GV3101 pMP90 harboring the p19 protein gene of tomato bushy stunt virus to repress silencing in plant cells (Voinnet *et al.*, 2003) and with *A. rhizogenes* 18r12v containing *mCherry* (Shaner *et al.*, 2004) fused to aquaporin AtPIP2A (Nelson *et al.*, 2007; Arabidopsis Biological Resource Center stock number CD3-1007; http://www.arabidopsis.org) that has been shown to localize to the plant plasma membrane (Cutler *et al.*, 2000). Leaf tissue was analyzed by confocal microscopy (Leica, http://www.leica.com/). Sodium chloride (1 M) was added to some specimens to induce plasmolysis to more clearly visualize localization of the GFP-GmUPS1 proteins to the plasma membrane.

GmUPS1-1 and GmUPS1-2 localization using *in situ* RT-PCR

For *in situ* RT-PCR localization experiments with *GmUPS1-1* and *GmUPS1-2*, mature nodules of 35-day-old soybean plants were fixed in FAA (10% v/v formaldehyde, 5% v/v acetic acid and 50% v/v ethanol), dehydrated and paraffin-embedded as previously described (Lee and Tegeder, 2004). Nodule sections (10 μm) were prepared and used for *in situ* RT-PCR analysis (Lee and Tegeder, 2004). Two primer sets were used that specifically amplified *GmUPS1-1* and *GmUPS1-2*, respectively (see Table S2). Amplification of 18S rRNA was used as a positive control, and negative controls were performed by omitting primers or Avian Myeloblastosis Virus (AMV) reverse transcriptase (Promega). The results were analyzed using light microscopy.

Production of *ex vitro* composite soybean plants and harvest of nodulated roots

Composite soybean plants expressing the *PvUPS1* promoter–RNAi *UPS1* or *PvUPS1* promoter–RNAi *GFP* (control) constructs in nodulated roots were produced as described previously (Collier *et al.*, 2005) but with some modifications to identify and remove non-transgenic roots at an early stage. In detail, decapitated 7-day-old soybean shoots were grown in Grodan cubes (Grodan, http://www.grodan.com/) inoculated with *A. rhizogenes* containing the specific constructs. After 2 weeks of growth, shoots with developed roots were removed from the cubes and adventitious roots were discarded, while putatively transgenic hairy roots originating from the teratoma region of the stem remained. The plants were then cultured in 50 ml polypropylene tubes with drainage holes (1 mm) containing Turface. After another 2 weeks of growth, individual roots of the RNAi plants were tested for successful transformation by using a lateral root for the GUS staining procedure, and non-transgenic roots were removed. To induce development of transgenic nodules, the remaining transgenic roots were then inoculated with *Bradyrhizobium japonicum* strain USDA110 by dipping the root system for 30 sec in an N-free nutrient solution (Lullien *et al.*, 1987) containing bacteria at OD_{600} = 0.08. Inoculated plants were transferred to 12.5 cm pots filled with water-saturated Turface growth medium. Plants were covered with clear, closed plastic bags overnight that were opened the following morning and removed 10 h later. The plants were grown in a walk-in growth chamber at 260 μmol photons m^{-2} sec^{-1} light intensity under the photoperiod, temperature and humidity conditions described above. After 30 days of growth, individual roots were harvested, and a lateral root sample was taken to test for transgenesis using the GUS assay. The confirmed transgenic nodulated roots were then photographed, and nodules and roots were sampled and stored at −80°C. Images were analyzed using ImageJ (Abramoff *et al.*, 2004) to determine nodule number and size.

PvUPS1 promoter–*GUS* composite plants were produced as described above, and nodules from hairy roots were analyzed by the GUS staining procedure (Jefferson *et al.*, 1987) to determine the location of GUS expression.

RNA extraction and expression analysis

RNA extraction and multiplex cDNA synthesis were performed as described by Kulcheski *et al.* (2010). Quantitative PCR primers were designed to determine the expression of genes involved in ureide synthesis (*ALN1–ALN4*, Duran and Todd, 2012; *UR9*, Takane *et al.*, 1997), ureide transport (*GmUPS1-1* and *GmUPS1-2*) and ammonium transport across the symbiosome membrane (*N-26*; Fortin *et al.*, 1987; Masalkar *et al.*, 2010). For accession numbers and primers, see Table S2. Amplification of microRNAs (miR156a, miR156b and miR1520d) was used as a control for relative quantification. These miRNAs have recently been demonstrated to have higher expression stability in soybean than commonly used, protein-coding housekeeping genes (Kulcheski *et al.*, 2010). Relative expression levels of genes were computed from C_t values as previously described (Sanders *et al.*, 2009).

Determining total ureide, allantoin and allantoic acid concentrations

To determine allantoin, allantoic acid and total ureide concentrations in nodules and roots, 5 mg of lyophilized tissue was used. Nodules were grouped by size into small (<1.59 mm in diameter), medium (1.59–1.98 mm diameter) and large (>1.98 mm diameter) nodules using a drill gauge (Irwin, http://www.irwin.com/). Nodule and root extracts were prepared from a pool of five to eight RNAi plants, from at least two transgenic roots per plant. The tissue was homogenized in 1 ml ice-cold H_2O, pipetted through Calbiochem Miracloth (EMD Chemicals, http://www.emdmillipore.com/chemicals) and centrifuged for 30 min at 4°C and 15 000 ***g***. The supernatant (100 μl) was used for total ureide and allantoic acid assays, respectively, according to a protocol kindly provided by Dr Cesar Arrese-Igor (Departamento de Ciencias del Medio Natural, Universidad Pública de Navarra, Pamplona, Spain). This protocol basically follows that described by Vogels and van der Drift (1970), but phosphate buffer was substituted with water for volume adjustment of samples. In addition, phenylhydrazine was added to samples in conjunction with 0.65 N HCl prior to instead of after the second boiling step, and concentrated HCl was cooled to −20°C rather than 0°C. Measured values for total ureides and allantoic acid were then used to calculate the allantoin content.

Acetylene reduction assay

Nitrogenase activity was determined using the acetylene reduction assay as described by House *et al.* (2004). Transgenic nodules were harvested from individual roots from at least 15 plants and grouped according to their size as described above. For the assay, 20 small, 10 medium or five large-sized nodules were placed at room temperature in 5 ml glass vials sealed with rubber septa (Chemglass, http://www.chemglass.com/). The headspace gas (250 μl) was replaced with acetylene, and a 250 μl gas sample was withdrawn after 20 min of incubation, and the ethylene produced was measured using a Shimadzu GC-8A gas chromatograph (Shimadzu, http://www.shimadzu.com/). Approximately 30 total measurements were performed for RNAi *UPS1* or RNAi control nodules. Acetylene reduction to ethylene was calculated as previously described (House *et al.*, 2004).

Structural analysis of nodules

Various sizes of nodules (described above) were fixed (4% glutaraldehyde, 2% paraformaldehyde, 50 mM PIPES buffer), embedded in London Resin White acrylic resin (Ted Pella, http://www.tedpella.com/), sectioned (1 μm) and stained with safranin as previously described (Harrington *et al.*, 1997). Stained sections were imaged by light microscopy using a Leica DM LFSA microscope equipped with a Leica DFC 300 FX cooled CCD camera.

Statistical analysis

Data are shown for one set of at least 16 RNAi *UPS1* and RNAi control plants, respectively, but are representative of at least two independently grown sets of plants. Results are from approximately

25–30 transgenic nodulated roots (including lateral roots), and are presented as means ± standard deviation. One-way analysis of variance (ANOVA) was used to determine statistical significance using SIGMASTAT 3.0 (Systat Software, http://www.systat.com/).

ACKNOWLEDGEMENTS

We acknowledge the support from our greenhouse manager Chuck Cody as well as the Franceschi Microscopy and Imaging Center at Washington State University. We are thankful to Nathan Tarlyn, Amanda Herbster and Dr Michael Kahn (Institute of Biological Chemistry at Washington State University) for helping with tissue preparation, localization studies and the acetylene reduction assay, respectively. We are grateful to Nathalie Walter for assisting with the harvests and data collection. This work was funded by US National Science Foundation grant IOS 0448506 and Agricultural and Food Research Initiative Competitive grant number 2010-65115-20382 from the US Department of Agriculture National Institute of Food and Agriculture.

SUPPORTING INFORMATION

Additional Supporting Information may be found in the online version of this article:

Figure S1. *PvUPS1* promoter analysis.

Table S1. Primers used for isolation of *GmUPS1-1* and *GmUPS1-2* and preparation of constructs.

Table S2. Primers used for *GmUPS1-1* and *GmUPS1-2 in situ* RT-PCR localization studies and for expression analyses of genes involved in nitrogen metabolism and transport.

Please note: As a service to our authors and readers, this journal provides supporting information supplied by the authors. Such materials are peer-reviewed and may be re-organized for online delivery, but are not copy-edited or typeset. Technical support issues arising from supporting information (other than missing files) should be addressed to the authors.

REFERENCES

Abaidoo, R.C., George, T., Bohlool, B.B. and Singleton, P.W. (1990) Influence of elevation and applied nitrogen on rhizosphere colonization and competition for nodule occupancy by different rhizobial strains on field grown soybean and common bean. *Can. J. Microbiol.* **36**, 92–96.

Abramoff, M., Magalhaes, P. and Ram, S. (2004) Image processing with ImageJ. *Biophotonics Int.* **11**, 36–42.

Alamillo, J.M., Díaz-Leal, J.L., Sánchez-Moran, M.V. and Pineda, M. (2010) Molecular analysis of ureide accumulation under drought stress in *Phaseolus vulgaris* L. *Plant, Cell Environ.* **33**, 1828–1837.

Atkins, C.A. and Smith, P.M. (2007) Translocation in legumes: assimilates, nutrients, and signaling molecules. *Plant Physiol.* **144**, 550–561.

de Beer, M., Krüger, G.H.J. and van Heerden, P.D.R. (2007) Biochemical changes in soybean root nodules during development and senescence-effects of dark chilling. *S. Afr. J. Bot.* **73**, 284–285.

Bergmann, H., Preddie, E. and Verma, D.P.S. (1983) Nodulin-35 – a subunit of specific uricase (uricase-II) induced and localized in the uninfected cells of soybean nodules. *EMBO J.* **2**, 2333–2339.

Bevan, M., Barnes, W.M. and Chilton, M.D. (1983) Structure and transcription of the nopaline synthase gene region of T-DNA. *Nucleic Acids Res.* **11**, 369–385.

Brown, S.M. and Walsh, K.B. (1994) Anatomy of the legume nodule cortex with respect of nodule permeability. *Aust. J. Plant Physiol.* **21**, 49–68.

Brown, S.M., Oparka, K.J., Sprent, J.I. and Walsh, K.B. (1995) Symplastic transport in soybean root nodules. *Soil Biol. Biochem.* **27**, 387–399.

Buss, G.R., Camper, H.M. Jr and Roane, C.W. (1988) Registration of 'Hutcheson' soybean. *Crop Sci.* **28**, 1024–1025.

Collier, R., Fuchs, B., Walter, N., Kevin Lutke, W. and Taylor, C.G. (2005) *Ex vitro* composite plants: an inexpensive, rapid method for root biology. *Plant J.* **43**, 449–457.

Combard, A., Brevet, J., Borowski, D., Cam, K. and Tempe, J. (1987) Physical map of the T-DNA region of *Agrobacterium rhizogenes* strain NCPPB2659. *Plasmid*, **18**, 70–75.

Cutler, S.R., Ehrhardt, D.W., Griffitts, J.S. and Somerville, C.R. (2000) Random GFP::cDNA fusions enable visualization of subcellular structures in cells of *Arabidopsis* at a high frequency. *Proc. Natl Acad. Sci. USA*, **97**, 3718–3723.

Datta, D.B., Triplett, E.W. and Newcomb, E.H. (1991) Localization of xanthine dehydrogenase in cowpea root nodules: implications for the interaction between cellular compartments during ureide biogenesis. *Proc. Natl Acad. Sci. USA*, **88**, 4700–4702.

Desimone, M., Catoni, E., Ludewig, U., Hilpert, M., Schneider, A., Kunze, R., Tegeder, M., Frommer, W.B. and Schumacher, K. (2002) A novel superfamily of transporters for allantoin and other oxo derivatives of nitrogen heterocyclic compounds in Arabidopsis. *Plant Cell*, **14**, 847–856.

Dohmen, R.J., Strasser, A.W., Honer, C.B. and Hollenberg, C.P. (1991) An efficient transformation procedure enabling long-term storage of competent cells of various yeast genera. *Yeast*, **7**, 691–692.

Duran, V.A. and Todd, C.D. (2012) Four allantoinase genes are expressed in nitrogen-fixing soybean. *Plant Physiol. Biochem.* **54**, 149–155.

Eaglesham, A.R.J. (1989) Nitrate inhibition of root nodule symbiosis in doubly rooted soybean plants. *Crop Sci.* **29**, 115–119.

Fortin, M.G., Morrison, N.A. and Verma, D.P.S. (1987) Nodulin 26, a peribacteroid membrane nodulin is expressed independently of the development of the peribacteroid compartment. *Nucleic Acids Res.* **15**, 813–824.

Froissard, M., Belgareh-Touzé, N., Buisson, N., Desimone, M., Frommer, W.B. and Haguenauer-Tsapis, R. (2006) Heterologous expression of a plant uracil transporter in yeast: improvement of plasma membrane targeting in mutants of the Rsp5p ubiquitin protein ligase. *Biotechnol. J.* **1**, 308–320.

Fujihara, S. and Yamaguchi, M. (1978) Effect of allopurinol [4-hydroxypyrazolo(3,4-d)pyrimidine] on the metabolism of allantoin in soybean plants. *Plant Physiol.* **62**, 134–138.

Fujikake, H., Yamazaki, A., Ohtake, N. *et al.* (2003) Quick and reversible inhibition of soybean root nodule growth by nitrate involves a decrease in sucrose supply to nodules. *J. Exp. Bot.* **54**, 1379–1388.

Gordon, A.J., Ryle, G.J.A., Mitchell, D.F. and Powell, C.E. (1985) The flux of ^{14}C labeled photosynthate through soybean root nodules during N_2 fixation. *J. Exp. Bot.* **36**, 756–769.

Green, L.S. and Emerich, D.W. (1997) The formation of nitrogen fixing bacteroids is delayed but not abolished in soybean infected by an α-ketoglutarate dehydrogenase deficient mutant of *Bradyrhizobium japonicum*. *Plant Physiol.* **114**, 1359–1368.

Guinel, F.C. (2009) Getting around the legume nodule: I. The structure of the peripheral zone in four nodule types. *Botany*, **87**, 1117–1138.

Hanks, J.F., Tolbert, N.E. and Schubert, K.R. (1981) Localization of enzymes of ureide biosynthesis in peroxisomes and microsomes of nodules. *Plant Physiol.* **68**, 65–69.

Harrington, G.N., Franceschi, V.R., Offler, C.E., Patrick, J.W., Tegeder, M., Frommer, W.B., Harper, J.F. and Hitz, W.D. (1997) Cell specific expression of three genes involved in plasma membrane sucrose transport in developing *Vicia faba* seed. *Protoplasma*, **197**, 160–173.

van Heerden, P.D.R., Kiddle, G., Pellny, T.K., Mokwala, P.W., Jordaan, A., Strauss, A.J., de Beer, M., Schlueter, U., Kunert, K.J. and Foyer, C.H. (2008) Regulation of respiration and the oxygen diffusion barrier in soybean protect symbiotic nitrogen fixation from chilling-induced inhibition and shoots from premature senescence. *Plant Physiol.* **148**, 316–327.

Helliwell, C.A., Wesley, S.V., Wielopolska, A.J. and Waterhouse, P.M. (2002) High-throughput vectors for efficient gene silencing in plants. *Funct. Plant Biol.* **29**, 1217–1225.

Herridge, D.F., Roughley, R.J. and Brockwell, J. (1984) Effect of rhizobia and soil nitrate on the establishment and functioning of the soybean symbiosis in the field. *Aust. J. Agric. Res.* **35**, 149–161.

Higo, K., Ugawa, Y., Iwamoto, M. and Higo, H. (1998) PLACE: a database of plant *cis*-acting regulatory DNA elements. *Nucleic Acids Res.* **26**, 358–359.

House, B.L., Mortimer, M.W. and Kahn, M.L. (2004) New recombination methods for *Sinorhizobium meliloti* genetics. *Appl. Environ. Microbiol.* **70**, 2806–2815.

Imsande, J. (1986) Inhibition of nodule development in soybean by nitrate or reduced nitrogen. *J. Exp. Bot.* **37**, 348–355.

James, E.K., Sprent, J.I., Minchin, F.R. and Brewin, N.J. (1991) Intercellular location of glycoprotein in soybean nodules – effect of altered rhizosphere oxygen concentration. *Plant, Cell Environ.* **14**, 467–476.

Jefferson, R.A., Kavanagh, T.A. and Bevan, M.W. (1987) GUS fusions: β-glucuronidase as a sensitive and versatile gene fusion marker in higher plants. *EMBO J.* **6**, 3901–3907.

Kahn, K. and Tipton, P. A. (1997) Kinetic mechanism and cofactor content of soybean root nodule urate oxidase. *Biochem.* **36**, 4731–4738.

King, C.A. and Purcell, L.C. (2005) Inhibition of N_2 fixation in soybean is associated with elevated ureides and amino acids. *Plant Physiol.* **137**, 1389–1396.

Kulcheski, F.R., Marcelino-Guimaraes, F.C., Nepomuceno, A.L., Abdelnoor, R.V. and Margis, R. (2010) The use of microRNAs as reference genes for quantitative polymerase chain reaction in soybean. *Anal. Biochem.* **406**, 185–192.

Ladrera, R., Marino, D., Larrainzar, E., Gonzalez, E.M. and Arrese-Igor, C. (2007) Reduced carbon availability to bacteroids and elevated ureides in nodules, but not in shoots, are involved in the nitrogen fixation response to early drought in soybean. *Plant Physiol.* **145**, 539–546.

Larrainzar, E., Wienkoop, S., Weckwerth, W., Ladrera, R., Arrese-Igor, C. and Gonzalez, E.M. (2007) *Medicago truncatula* root nodule proteome analysis reveals differential plant and bacteroid responses to drought stress. *Plant Physiol.* **144**, 1495–1507.

Lee, Y.H. and Tegeder, M. (2004) Selective expression of a novel high-affinity transport system for acidic and neutral amino acids in the tapetum cells of *Arabidopsis* flowers. *Plant J.* **40**, 60–74.

Libault, M., Joshi, T., Takahashi, K. *et al.* (2009) Large-scale analysis of putative soybean regulatory gene expression identifies a *Myb* gene involved in soybean nodule development. *Plant Physiol.* **151**, 1207–1220.

Libault, M., Govindarajulu, M., Berg, R.H., Ong, Y.T., Puricelli, K., Taylor, C.G., Xu, D. and Stacey, G. (2011) A dual-targeted soybean protein is involved in *Bradyrhizobium japonicum* infection of soybean root hair and cortical cells. *Mol. Plant Microbe Interact.* **24**, 1051–1060.

Livak, K. J. and Schmittgen, T. D. (2001) Analysis of relative gene expression data using real-time quantitative PCR and the $2^{-(\Delta\Delta\ CT)}$. *Methods*, **25**, 402–408.

Lullien, V., Barker, D.G., Lajudie, P.d. and Huguet, T. (1987) Plant gene expression in effective and ineffective root nodules of alfalfa (*Medicago sativa*). *Plant Mol. Biol.* **9**, 469–478.

Masalkar, P., Wallace, I.S., Hwang, J.H. and Roberts, D.M. (2010) Interaction of cytosolic glutamine synthetase of soybean root nodules with the C-terminal domain of the symbiosome membrane Nodulin 26 aquaglyceroporin. *J. Biol. Chem.* **285**, 23880–23888.

Maunoury, N., Kondorosi, A., Kondorosi, E. and Mergaert, P. (2008) Cell biology of nodule infection and development. In *Nitrogen-fixing Leguminous Symbioses* (Dilworth, M.J., James, E.K., Sprent, J.I. and Newton, W.E., eds). Dordrecht: Springer, pp. 153–189.

McClure, P.R. and Israel, D.W. (1979) Transport of nitrogen in the xylem of soybean plants. *Plant Physiol.* **64**, 411–416.

McCormac, A.C., Elliott, M.C. and Chen, D.F. (1998) A simple method for the production of highly competent cells of *Agrobacterium* for transformation via electroporation. *Mol. Biotechnol.* **9**, 155–159.

Morey, K.J., Ortega, J.L. and Sengupta-Gopalan, C. (2002) Cytosolic glutamine synthetase in soybean is encoded by a multigene family, and the members are regulated in an organ-specific and developmental manner. *Plant Physiol.* **128**, 182–193.

Nelson, B.K., Cai, X. and Nebenfuhr, A. (2007) A multicolored set of *in vivo* organelle markers for co-localization studies in Arabidopsis and other plants. *Plant J.* **51**, 1126–1136.

Newcomb, E.H., Kaneko, Y. and VandenBosch, K.A. (1989) Specialization of the inner cortex for ureide production in soybean root nodules. *Protoplasma*, **150**, 150–159.

Obermeyer, G. and Tyerman, S.D. (2005) NH_4^+ currents across the peribacteroid membrane of soybean. Macroscopic and microscopic properties, inhibition by Mg2+, and temperature dependence indicate a subpicoSiemens channel finely regulated by divalent cations. *Plant Physiol.* **139**, 1015–1029.

Parsons, R. and Day, D.A. (1990) Mechanism of soybean nodule adaptation to different oxygen pressures. *Plant, Cell Environ.* **13**, 501–512.

Pate, J.S., Gunning, B.E.S. and Briarty, L.G. (1969) Ultrastructure and functioning of the transport system of the leguminous root nodule. *Planta*, **85**, 11–34.

Pélissier, H.C. and Tegeder, M. (2007) PvUPS1 plays a role in source–sink transport of allantoin in French bean (*Phaseolus vulgaris*). *Funct. Plant Biol.* **34**, 282–291.

Pélissier, H.C., Frerich, A., Desimone, M., Schumacher, K. and Tegeder, M. (2004) PvUPS1, an allantoin transporter in nodulated roots of French bean. *Plant Physiol.* **134**, 664–675.

Perera, J. and Rice, S. (2002) Composition and methods for the modification of gene expression. United States Patent number US 6,380,459 B1.

Purcell, L.C. and Sinclair, T.R. (1990) Nitrogenase activity and nodule gas permeability response to rhizospheric NH_3 in soybean. *Plant Physiol.* **92**, 268–272.

Raikhel, N. (1992) Nuclear targeting in plants. *Plant Physiol.* **100**, 1627–1632.

Rainbird, R.M. (1982) Elements in the cost of nitrogen fixation with special reference to the legume cowpea (*Vigna unguiculata* (L.) Walp. cv. Caloona). PhD Thesis. The University of Western Australia, Australia.

Rainbird, R.M., Thorne, J.H. and Hardy, R.W. (1984) Role of amides, amino acids, and ureides in the nutrition of developing soybean seeds. *Plant Physiol.* **74**, 329–334.

Rentsch, D., Laloi, M., Rouhara, I., Schmelzer, E., Delrot, S. and Frommer, W.B. (1995) *NTR1* encodes a high affinity oligopeptide transporter in *Arabidopsis*. *FEBS Lett.* **370**, 264–268.

Sanders, A., Collier, R., Trethewy, A., Gould, G., Sieker, R. and Tegeder, M. (2009) AAP1 regulates import of amino acids into developing *Arabidopsis* embryos. *Plant J.* **59**, 540–552.

Schmidt, A., Su, Y.H., Kunze, R., Warner, S., Hewitt, M., Slocum, R.D., Ludewig, U., Frommer, W.B. and Desimone, M. (2004) UPS1 and UPS2 from *Arabidopsis* mediate high affinity transport of uracil and 5-fluorouracil. *J. Biol. Chem.* **279**, 44817–44824.

Schmidt, A., Baumann, N., Schwarzkopf, A., Frommer, W.B. and Desimone, M. (2006) Comparative studies on ureide permeases in *Arabidopsis thaliana* and analysis of two alternative splice variants of AtUPS5. *Planta*, **224**, 1329–1340.

Schmutz, J., Cannon, S.B., Schlueter, J. *et al.* (2010) Genome sequence of the palaeopolyploid soybean. *Nature*, **463**, 178–183.

Schubert, K.R. (1981) Enzymes of purine biosynthesis and catabolism in *Glycine max*. I. Comparison of activities with N2 fixation and composition of xylem exudate during nodule development. *Plant Physiol.* **68**, 1115–1122.

Selker, J.M.L. (1988) 3-Dimensional organization of uninfected tissue in soybean root nodules and its relation to cell specialization in the central region. *Protoplasma*, **147**, 178–190.

Selker, J.M.L. and Newcomb, E.H. (1985) Spatial relationships between uninfected and infected cells in root nodules of soybean. *Planta*, **165**, 446–454.

Serraj, R., Sinclair, T.R. and Purcell, L.C. (1999a) Symbiotic N_2 fixation response to drought. *J. Exp. Bot.* **50**, 143–155.

Serraj, R., Vadez, V.V., Denison, R.F. and Sinclair, T.R. (1999b) Involvement of ureides in nitrogen fixation inhibition in soybean. *Plant Physiol.* **119**, 289–296.

Serraj, R., Vadez, V. and Sinclair, T.R. (2001) Feedback regulation of symbiotic N_2 fixation under drought stress. *Agronomie*, **21**, 621–626.

Shaner, N.C., Campbell, R.E., Steinbach, P.A., Giepmans, B.N., Palmer, A.E. and Tsien, R.Y. (2004) Improved monomeric red, orange and yellow fluorescent proteins derived from *Discosoma* sp. red fluorescent protein. *Nat. Biotechnol.* **22**, 1567–1572.

Siemering, K.R., Golbik, R., Sever, R. and Haseloff, J. (1996) Mutations that suppress the thermosensitivity of green fluorescent protein. *Curr. Biol.* **6**, 1653–1663.

de Silva, M., Purcell, L.C. and King, C.A. (1996) Soybean petiole ureide response to water deficits and decreased transpiration. *Crop Sci.* **36**, 611–616.

Sinclair, T.R. and Serraj, R. (1995) Legume nitrogen fixation and drought. *Nature*, **378**, 344.

Smith, P.M. and Atkins, C.A. (2002) Purine biosynthesis. Big in cell division, even bigger in nitrogen assimilation. *Plant Physiol.* **128**, 793–802.

Smith, P.M., Winter, H., Storer, P.J., Bussell, J.D., Schuller, K.A. and Atkins, C.A. (2002) Effect of short-term N_2 deficiency on expression of the ureide pathway in cowpea root nodules. *Plant Physiol.* **129**, 1216–1221.

Sparkes, I.A., Runions, J., Kearns, A. and Hawes, C. (2006) Rapid, transient expression of fluorescent fusion proteins in tobacco plants and generation of stably transformed plants. *Nat. Protoc.* **1**, 2019–2025.

Stacey, G., Vodkin, L., Parrott, W.A. and Shoemaker, R.C. (2004) National Science Foundation-sponsored workshop report. Draft plan for soybean genomics. *Plant Physiol.* **135**, 59–70.

Streeter, J.G. (1979) Allantoin and allantoic acid in tissues and stem exudate from field-grown soybean plants. *Plant Physiol.* **63**, 478–480.

Streeter, J.G. (1992) Analysis of apoplastic solutes in the cortex of soybean nodules. *Physiol. Plant.* **84**, 584–592.

Streeter, J.G. (1993) Translocation – a key factor limiting the efficiency of nitrogen fixation in legume nodules. *Physiol. Plant.* **87**, 616–623.

Streeter, J.G. (2003) Effects of drought on nitrogen fixation in soybean root nodules. *Plant, Cell Environ.* **26**, 1199–1204.

Streeter, J.G. and Salminen, S.O. (1993) Alterations in apoplastic and total solute concentrations in soybean nodules resulting from treatments known to affect gas diffusion. *J. Exp. Bot.* **44**, 821–828.

Subramanian, S., Hu, X., Lu, G., Odelland, J.T. and Yu, O. (2004) The promoters of two isoflavone synthase genes respond differentially to nodulation and defense signals in transgenic soybean roots. *Plant Mol. Biol.* **54**, 623–639.

Subramanian, S., Stacey, G. and Yu, O. (2006) Endogenous isoflavones are essential for the establishment of symbiosis between soybean and *Bradyrhizobium japonicum*. *Plant J.* **48**, 261–273.

Takane, K., Tajima, S. and Kouchi, H. (1997) Two distinct uricase II (nodulin 35) genes are differentially expressed in soybean plants. *Mol. Plant-Microbe Interact.* **10**, 735–741.

Todd, C.D., Tipton, P.A., Blevins, D.G., Piedras, P., Pineda, M. and Polacco, J.C. (2006) Update on ureide degradation in legumes. *J. Exp. Bot.* **57**, 5–12.

Vadez, V. and Sinclair, T.R. (2000) Ureide degradation pathways in intact soybean leaves. *J. Exp. Bot.* **51**, 1459–1465.

Vadez, V. and Sinclair, T.R. (2001) Leaf ureide degradation and N_2 fixation tolerance to water deficit in soybean. *J. Exp. Bot.* **52**, 153–159.

Vadez, V., Sinclair, T.R. and Serraj, R. (2000) Asparagine and ureide accumulation in nodules and shoots as feedback inhibitors of N_2 fixation in soybean. *Physiol. Plant.* **110**, 215–223.

Van Dao, T., Nomura, M., Hamaguchi, R. *et al.* (2008) NAD-malic enzyme affects nitrogen fixing activity of *Bradyrhizobium japonicum* USDA 110 bacteroids in soybean nodules. *Microbes Environ.* **23**, 215–220.

VandenBosch, K.A. and Newcomb, E.H. (1986) Immunogold localization of nodule-specific uricase in developing soybean root nodules. *Planta*, **167**, 425–436.

Vauclare, P., Bligny, R., Gout, E., De Meuron, V. and Widmer, F. (2010) Metabolic and structural rearrangement during dark-induced autophagy in soybean (*Glycine max* L.) nodules: an electron microscopy and ^{31}P and ^{13}C nuclear magnetic resonance study. *Planta*, **231**, 1495–1504.

Veena, V. and Taylor, C.G. (2007) *Agrobacterium rhizogenes*: recent developments and promising applications. *In Vitro Cell. Dev. Biol. Plant*, **43**, 383–403.

Vogels, G.D. and van der Drift, C. (1970) Differential analyses of glyoxylate derivatives. *Anal. Biochem.* **33**, 143–157.

Voinnet, O., Rivas, S., Mestre, P. and Baulcombe, D. (2003) An enhanced transient expression system in plants based on suppression of gene silencing by the p19 protein of tomato bushy stunt virus. *Plant J.* **33**, 949–956.

Walsh, K.B. (1995) Physiology of the legume nodule and its response to stress. *Soil Biol. Biochem.* **27**, 637–655.

Walsh, K.B., McCully, M.E. and Canny, M.J. (1989) Vascular transport and soybean nodule function: nodule xylem is a blind alley, not a throughway. *Plant, Cell Environ.* **12**, 395–405.

Webb, J. and Sheehy, J.E. (1991) Legume nodule morphology with regard to oxygen diffusion and nitrogen fixation. *Ann. Bot.* **67**, 77–83.

Werner, A.K. and Witte, C.P. (2011) The biochemistry of nitrogen mobilization: purine ring catabolism. *Trends Plant Sci.* **16**, 381–387.

Werner, A.K., Sparkes, I.A., Romeis, T. and Witte, C.P. (2008) Identification, biochemical characterization, and subcellular localization of allantoate amidohydrolases from Arabidopsis and soybean. *Plant Physiol.* **146**, 418–430.

